

THE TRIPLE-REGGE TRIANGLE ANOMALY *

Alan. R. White[†]

High Energy Physics Division
Argonne National Laboratory
9700 South Cass, Il 60439, USA.

Abstract

It is shown that the U(1) triangle anomaly is present, as an infra-red divergence, in the six-reggeon triple-regge interaction vertex obtained from a maximally non-planar Feynman diagram in the full triple-regge limit of three-to-three quark scattering. An asymptotic dispersion relation multi-regge formalism can be used to isolate all anomaly contributions and to discuss when and how there is a cancelation.

*Work supported by the U.S. Department of Energy, Division of High Energy Physics, Contracts W-31-109-ENG-38 and DEFG05-86-ER-40272

[†]arw@hep.anl.gov

1. INTRODUCTION

In a companion paper to this[1] we have demonstrated that in massless QCD certain reggeized gluon interactions contain an infra-red divergence that can be understood as the infra-red appearance[2] of the U(1) quark anomaly. Such vertices appear in a wide variety of multi-regge reggeon diagrams[3] and so this is a potential new manifestation of the anomaly, in a dynamical role. In this paper we illustrate the results of [1] by presenting an abbreviated version of the central calculation. We study the full triple-regge limit[4] of three-to-three quark scattering and show that the anomaly is present in the (six-reggeon) triple-regge interaction vertex obtained from a “maximally non-planar” Feynman diagram. In [1] we also use an asymptotic dispersion relation formalism[5, 6] to show that the anomaly does not occur in other diagrams and to discuss cancelations among the maximally non-planar diagrams. In the latter half of this paper we give a very brief review of this formalism and the arguments involved. When the scattering states are elementary quarks or gluons the anomaly does indeed cancel. (It cancels in individual lowest-order diagrams after the transverse momentum integrations are performed.)

Since high-energy is involved, regge limits are a-priori close to perturbation theory at large transverse momentum, while in the infra-red region very strong constraints from analyticity and t -channel unitarity[5, 7] must also be satisfied. In perturbation theory (when gluons and quarks are massive) unitarity is satisfied by reggeon diagrams containing reggeized gluons and quarks[8]. In [3] we outlined a program to show that, in the massless theory, infra-red divergences produce a transition from perturbative reggeon diagrams to diagrams containing hadrons and the pomeron. In that paper we assumed the existence of the anomaly together with a number of properties that the results of [1] show to be essentially correct, although there are significant differences.

We study the three-to-three scattering process illustrated in Fig. 1(a)

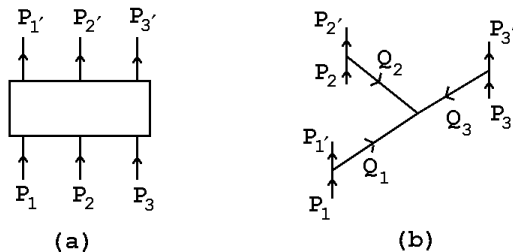


Fig. 1 Three-to-Three Scattering.

and define momentum transfers Q_1, Q_2 and Q_3 as in Fig. 1(b). The full triple-regge

limit[4] can be realized by taking each of P_1 , P_2 and P_3 large along distinct light-cones, with Q_1, Q_2 and Q_3 fixed, i.e.

$$\begin{aligned}
 P_1 \rightarrow P_1^+ &= (p_1, p_1, 0, 0), & p_1 \rightarrow \infty & & Q_1 &\rightarrow (\hat{q}_1, \hat{q}_1, q_{12}, q_{13}) \\
 P_2 \rightarrow P_2^+ &= (p_2, 0, p_2, 0), & p_2 \rightarrow \infty & & Q_2 &\rightarrow (\hat{q}_2, q_{21}, \hat{q}_2, q_{23}) \\
 P_3 \rightarrow P_3^+ &= (p_3, 0, 0, p_3), & p_3 \rightarrow \infty & & Q_3 &\rightarrow (\hat{q}_3, q_{31}, q_{32}, \hat{q}_3)
 \end{aligned} \tag{1}$$

Momentum conservation requires that

$$\hat{q}_1 + \hat{q}_2 + \hat{q}_3 = 0, \quad \hat{q}_1 + q_{21} + q_{31} = 0, \quad \hat{q}_2 + q_{12} + q_{32} = 0, \quad \hat{q}_3 + q_{13} + q_{23} = 0 \tag{2}$$

and so there are a total of five independent q variables which, along with p_1, p_2 and p_3 , give the necessary eight variables.

Consider the maximally non-planar Feynman diagram shown in Fig. 2, which gives contributions to the scattering of Fig. 1, as illustrated.

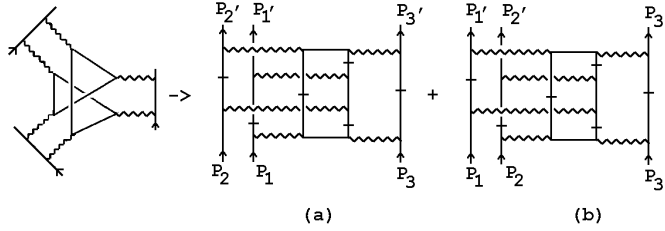


Fig. 2 Contributions from a Maximally Non-Planar Diagram

We ignore color factors until we discuss cancelations. In both Fig. 2(a) and (b) the hatched lines can clearly be close to mass-shell during the scattering. (If we sum over quark directions, the loop lines hatched in Fig. 2(a) are the unhatched lines in Fig. 2(b).) In either case, if we put all hatched lines on-shell and use the corresponding δ -functions to carry out longitudinal integrations in each of the external loops, we obtain a contribution to the lowest-order six-reggeon interaction as follows.

For Fig. 2(a) we label the gluon momenta as shown in Fig. 3(a).

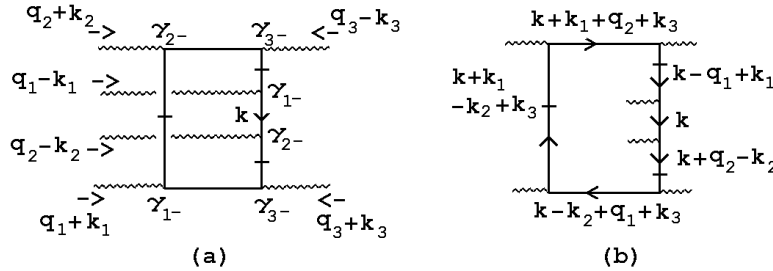


Fig. 3 (a) Gluon Momenta and γ -Matrix Couplings (b) Quark Loop Momenta

In the limit (1), the gluons exchanged by each of the fast quarks couple to the quark loop via a corresponding “light-like” γ -matrix that we have also shown in Fig. 3(a), i.e. $P_i^+ \rightarrow \gamma_{i-} = \gamma_0 - \gamma_i, i = 1, 2, 3$. To carry out the longitudinal k_3 integrations we use conventional light-cone co-ordinates. For the k_1 and k_2 integrations we use special light-cone co-ordinates[1], i.e. for a general four-momentum $p^\mu = (p_0, p_1, p_2, p_3)$ we write

$$p^\mu = p_{2-} \underline{n}_{1+} + p_{1-} \underline{n}_{2+} + \underline{p}_{12+}, \quad \begin{aligned} \underline{p}_{12+} &= p_{12-} \underline{n}_{12+} + p_3 \underline{n}_3 \\ p_{12-} &= p_1 + p_2 - p_0 \end{aligned} \quad (3)$$

where

$$\underline{n}_{1+} = (1, 1, 0, 0), \quad \underline{n}_{2+} = (1, 0, 1, 0), \quad \underline{n}_{12+} = (1, 1, 1, 0), \quad \underline{n}_3 = (0, 0, 0, 1) \quad (4)$$

Analogous decompositions to (3) can also be introduced for γ -matrices.

With the hatched lines on-shell the quark loop reduces to a triangle diagram. With the light-cone co-ordinates we have chosen only the momentum routing of Fig. 3(b) produces local components for all three vertices[1]. The local couplings, which are a prerequisite for the anomaly to be present, are calculated as follows.

$$\begin{aligned} & \int dk_{12-} \delta\left((k_1 + k - q_1)^2 - m^2\right) \gamma_{3-} \left((k_1 + k - q_1) \cdot \gamma + m\right) \gamma_{1-} \\ &= \int dk_{12-} \delta\left(k_{1-} k_{12-} + \dots\right) \gamma_{3-} \left(k_{1-} \cdot \gamma_{2-} + \dots\right) \gamma_{1-} = \gamma_{3-} \gamma_{2-} \gamma_{1-} + \dots \end{aligned} \quad (5)$$

$$\int dk_{21-} \delta\left((k_2 - k - q_2)^2 - m^2\right) \gamma_{2-} \left((k_2 - k - q_2) \cdot \gamma + m\right) \gamma_{3-} = \gamma_{2-} \gamma_{1-} \gamma_{3-} + \dots \quad (6)$$

$$\begin{aligned} & \int dk_{33+} \delta\left((k_3 + k + k_1 - k_2)^2 - m^2\right) \gamma_{1-} \left((k_3 + k + k_1 - k_2) \cdot \gamma + m\right) \gamma_{2-} \\ &= \gamma_{1-} \gamma_{3+} \gamma_{2-} + \dots \end{aligned} \quad (7)$$

In each case the dots indicate the contribution of additional non-local couplings.

Apart from a normalization factor, the asymptotic amplitude obtained is

$$\begin{aligned} & g^{12} \frac{p_1 p_2 p_3}{m^3} \times \\ & \int \frac{d^2 \underline{k}_{112+}}{(q_1 + \underline{k}_{112+})^2 (q_1 - \underline{k}_{112+})^2} \int \frac{d^2 \underline{k}_{212}}{(q_2 + \underline{k}_{212+})^2 (q_2 - \underline{k}_{212+})^2} \int \frac{d^2 \underline{k}_{33\perp}}{(q_3 + \underline{k}_{33\perp})^2 (q_3 - \underline{k}_{33\perp})^2} \\ & \int d^4 k \frac{Tr\{\hat{\gamma}_{12}(\not{k} + \not{k}_1 + \not{q}_2 + \not{k}_3 + m) \hat{\gamma}_{31}(\not{k} + m) \hat{\gamma}_{23}(\not{k} - \not{k}_2 + \not{q}_1 + \not{k}_3 + m)\}}{([k + k_1 + q_2 + k_3]^2 - m^2)(k^2 - m^2)([k - k_2 + q_1 + k_3]^2 - m^2)} + \dots \end{aligned} \quad (8)$$

where $k_{11-} = k_{22-} = k_{33-} = 0$, k_{12-} , k_{21-} and k_{33+} are determined by the δ -functions in (5)-(7) and

$$\begin{aligned}\hat{\gamma}_{31} &= \gamma_3 \gamma_2 \gamma_1 = \gamma^{-,+,-} - i \gamma_5 \gamma^{-,-,-} \\ \hat{\gamma}_{23} &= \gamma_2 \gamma_1 \gamma_3 = \gamma^{+,-,-} - i \gamma_5 \gamma^{-,-,-} \\ \hat{\gamma}_{12} &= \gamma_1 \gamma_3 \gamma_2 = \gamma^{-,-,-} + i \gamma_5 \gamma^{-,-,+}\end{aligned}\tag{9}$$

with

$$\gamma^{\pm,\pm,\pm} = \gamma^\mu \cdot n_\mu^{\pm,\pm,\pm}, \quad n^{\pm,\pm,\pm\mu} = (1, \pm 1, \pm 1, \pm 1)\tag{10}$$

That part of the amplitude not shown explicitly in (8) contains non-local couplings at one, or more, vertices of the quark triangle diagram.

The transverse momentum integrals and gluon propagators in (8) can be interpreted[1, 3] as the lowest-order contributions of two-reggeon states in each t_i ($= Q_i^2$)-channel. Removing these factors, the three γ_5 couplings in (9) give the $m = 0$ reggeon interaction

$$\begin{aligned}\Gamma_6(q_1, q_2, q_3, \tilde{k}_1, \tilde{k}_2, k_{3\perp}, 0) = \\ \int d^4k \frac{Tr\{\gamma_5 \gamma_{-,-,+}(\not{k} + \not{k}_1 + \not{q}_2 + \not{k}_3) \gamma_5 \gamma_{-,-,-} \not{k} \gamma_5 \gamma_{-,-,-}(\not{k} - \not{k}_2 + \not{q}_1 + \not{k}_3)\}}{(k + k_1 + q_2 + k_3)^2 k^2 (k - k_2 + q_1 + k_3)^2} + \dots\end{aligned}\tag{11}$$

This interaction corresponds to the triangle diagram of Fig. 4.

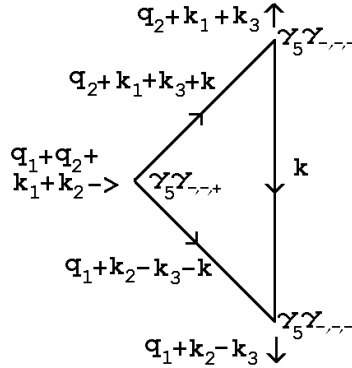


Fig. 4 The Triangle Diagram Corresponding to (11)

To obtain the maximal anomaly infra-red divergence[1, 2] we must have a component of the axial-vector triangle diagram tensor $\Gamma^{\mu\nu\lambda}$ with $\mu = \nu$ having a lightlike projection and λ an orthogonal index having a spacelike projection. This requirement is met by (11) if the light-like projection is made on either \underline{n}_{1+} or \underline{n}_{2+} . In each case, $\gamma^{-,-,+}$ has the necessary orthogonal spacelike component. The anomaly divergence[1, 2] will

then appear if we can take the limit

$$(k_1 + q_2 + k_3)^2 \sim (q_1 + q_2 + k_1 + k_2)^2 \sim (k_2 + q_1 - k_3)^2 \sim \mathbf{q}^2 \rightarrow 0 \quad (12)$$

of (11) while keeping a finite light-like momentum, parallel to either \underline{n}_{1-} or \underline{n}_{2+} , flowing through the diagram. The mass-shell constraints of (5) - (7) must also be satisfied.

We first show that the limiting configuration in which $\mathbf{q} = 0$ can be realized, with the loop momentum $k \sim \mathbf{q} = 0$. It is then straightforward to add momenta that are $O(\mathbf{q})$ so that the limit (12) can be taken. To satisfy (12) we impose

$$q_1 + q_2 + k_1 + k_2 = 0, \quad q_1 + k_2 - k_3 = (2l, -2l, 0, 0) \sim \underline{n}_{1-} \quad (13)$$

If we take $q_1 - k_1$ and $q_2 - k_2$ lightlike with

$$q_{12-} = -k_{12-} = l, \quad q_{21-} = -k_{21-} = -l, \quad \underline{q}_{112+} = \underline{k}_{112+} = -\underline{q}_{212+} = -\underline{k}_{212+} \quad (14)$$

then the first condition in (13) and the δ -functions of (5) and (6) are satisfied and $q_3 = -q_1 - q_2 = (0, l, -l, 0)$ has the necessary spacelike form. The second condition of (13) then requires $k_3 = (0, 3l, l, 0)$, while the δ -function of (7) requires

$$8 l q_{112-} = q_1^2 = \underline{q}_{112+}^2 = q_{112-}^2 + q_{13}^2 \quad (15)$$

All requirements are satisfied, therefore, with

$$(q_1 + k_1)^2 = 4q_1^2 = (q_2 + k_2)^2 = 4q_2^2 = 32 l q_{112-} = \frac{32}{\sqrt{2}} (q_3^2)^{1/2} (q_1^2 - q_{13}^2)^{1/2} \quad (16)$$

Adding momenta $O(\mathbf{q})$ parallel to \underline{n}_{12-} , the limit $\mathbf{q} \rightarrow 0$, with l fixed, gives

$$(q_1 - k_1)^2 \sim (q_2 - k_2)^2 \sim \mathbf{q}^2 \rightarrow 0 \quad (17)$$

while

$$(q_1 + k_1)^2 \rightarrow (q_2 + k_2)^2 \not\rightarrow 0, \quad (q_3 - k_3)^2 \rightarrow 2(q_3 + k_3)^2 \not\rightarrow 0 \quad (18)$$

and the six-reggeon vertex Γ_6 has the divergence

$$\Gamma_6 \sim \epsilon_{\underline{n}_{1+}, \underline{n}_3, \underline{n}_{2+}, \underline{n}_{12+}} \frac{l^2}{\mathbf{q}} \sim \frac{Q_3^2}{\mathbf{q}} \quad (19)$$

The singular behavior (19) occurs when $Q_3^2 \neq 0$ and $Q_1^2 = Q_2^2 \neq 0$. However, (16) allows $Q_1^2 = Q_2^2 \rightarrow 0$ with $q_{12-} \sim q_{21-} \sim \sqrt{Q_3^2} \neq 0$. That the anomaly divergence

persists when $Q_1^2 = Q_2^2 \rightarrow 0$ is important for identifying its occurrence when a helicity-flip limit[1] is taken, in addition to the triple-regge limit.

If, in the previous discussion, we instead impose

$$q_2 + k_1 + k_3 = (2l, 0, -2l, 0) \sim \underline{n}_{2-} \quad (20)$$

the role of 1 and 2 is interchanged and (19) is replaced by

$$\Gamma_6 \sim \epsilon_{\underline{n}_{2+}, \underline{n}_3, \underline{n}_{1+}, \underline{n}_{12+}} \frac{l^2}{q} \quad (21)$$

However, the singular configuration for (21) differs from that for (19) by $k_3 \leftrightarrow -k_3$, in addition to $1 \leftrightarrow 2$. Therefore, although $Q_1^2 = Q_2^2$ in both cases, the antisymmetry of the ϵ -tensor does not produce a cancellation of the two divergences within the reggeon vertex Γ_6 . In the full hatched diagram of Fig. 2(a), both (19) and (21) will contribute and, since the integration over k_3 in (8) is symmetric, there will be a cancelation after integration. Clearly the contribution from Fig. 2(b) can be discussed in exact parallel with our discussion of Fig. 2(a).

In higher-orders the two gluons in each t_i channel are replaced by even signature two-reggeon states with couplings G_1, G_2 and G_3 to the external scattering states. If we keep the same quark loop interaction, the amplitude with even signature in each channel is obtained by summing over all diagrams related by a twist, as in Fig. 5 and in each case keeping the two contributions corresponding to Figs.2(a) and (b). Both the color factors and all three of the k_i -integrations are then symmetric and the anomaly cancels. Sufficient antisymmetry to avoid cancelation would appear only if all three reggeon states had anomalous color parity (\neq signature). However, such reggeon states do not couple to elementary scattering quarks (or gluons),

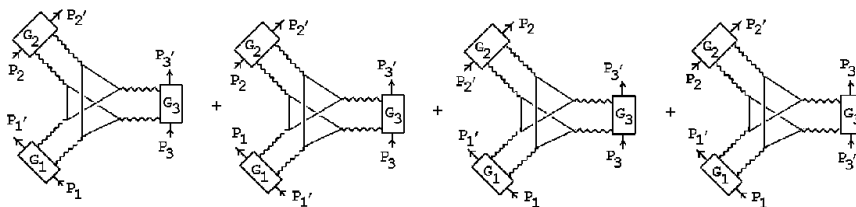


Fig. 5 The Sum of Twisted Diagrams

We have not discussed whether other combinations of hatched lines in the diagram of Fig. 2 could produce contributions to the reggeon interaction which also contain the anomaly. A more difficult problem, a-priori, is to determine whether there are contributions to the six-reggeon interaction by other Feynman diagrams that are

not of the maximally non-planar type. In higher-orders, as both quarks and gluons reggeize, we expect the full non-planarity property to be necessary to produce, in each regge channel, the double spectral function property that is well-known to be required for regge cut couplings. In lowest-order we can not appeal to this expectation and, a-priori, all diagrams of the form illustrated in Fig. 6 have the quark loop needed to produce the anomaly [1, 2],

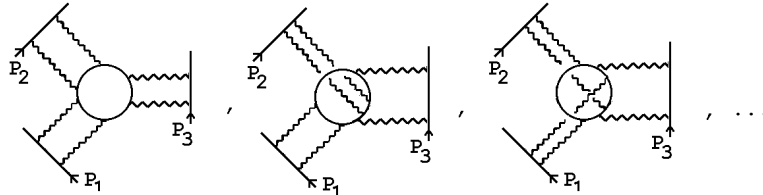


Fig. 6 Quark Scattering Diagrams with Two Gluons in each t_i -channel.

The total number of diagrams of this form is $O(100)$ and so studying them individually would clearly be difficult, if not impossible.

Fortunately we are able to systematically count all anomaly contributions by using the multi-regge asymptotic dispersion relation formalism developed in [5] and [6]. In the triple-regge limit “bad boundary-values” are hidden[5, 6] and the asymptotic cut structure of amplitudes is that of normal threshold branch-cuts satisfying the Steinmann relations, i.e. no double discontinuities in overlapping channels. Consequently the full amplitude can be written as

$$M(P_1, P_2, P_3, Q_1, Q_2, Q_3) = \sum_{\mathcal{C}} M^{\mathcal{C}}(P_1, P_2, P_3, Q_1, Q_2, Q_3) + M^0, \quad (22)$$

where M^0 contains all non-leading triple-regge behavior, double-regge behavior, etc. and the sum is over all triplets \mathcal{C} of three non-overlapping, asymptotically distinct, cuts allowed by the Steinmann relations.

For each \mathcal{C} , say $\mathcal{C} = (s_1, s_2, s_3)$, we write

$$M^{\mathcal{C}}(P_1, P_2, P_3, Q_1, Q_2, Q_3) = \frac{1}{(2\pi i)^3} \int ds'_1 ds'_2 ds'_3 \frac{\Delta^{\mathcal{C}}(\underline{t}, \underline{u}, s'_1, s'_2, s'_3)}{(s'_1 - s_1)(s'_2 - s_2)(s'_3 - s_3)} \quad (23)$$

$$\{s_i > s_{i0}, \forall i\}$$

where $\Delta^{\mathcal{C}}$ is the triple discontinuity

$$\Delta^{\mathcal{C}}(\underline{t}, \underline{u}, s_1, s_2, s_{n-3}) = \sum_{\epsilon} (-1)^{\epsilon} M(\underline{t}, \underline{u}, s_1 \pm i0, s_2 \pm i0, s_3 \pm i0), \quad (24)$$

where u_1 and u_2 are appropriate azimuthal angular variables. The sum over ϵ is over all combinations of $+$ and $-$ signs. The s_{i0} are finite, but arbitrary, values of the s_i . Because of the Steinmann relations, Δ^C contains only normal phase-space integrals. This implies that we appropriately evaluate multiple discontinuities of Feynman diagrams by simply putting corresponding lines on mass-shell.

Using tree diagrams, in which an internal line represents a channel discontinuity, all the triple discontinuities are of one of the two forms illustrated in Fig. 7.

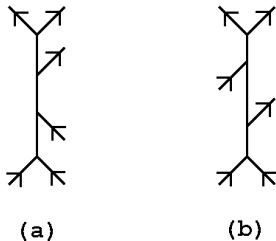


Fig. 7 Tree Diagrams for Triple Discontinuities.

Both contain initial and final state subenergy discontinuities and are distinguished by whether the third discontinuity is in the total energy, as in Fig. 7(a), or in a cross-energy, as in Fig. 7(b). Since there are six possible combinations of initial and final subenergies, there are twelve triple discontinuities in each physical region. Four physical regions provide a total of forty-eight triple discontinuities, twenty-four of each kind, contributing to the dispersion relation.

The multi-regge Sommerfeld-Watson representations[1] are quite different for the two types of triple discontinuities. It is possible to show from the resulting kinematic structure that the anomaly can appear only in the (a) type. Therefore, it does not appear in the inclusive cross-sections obtained from the (b) type via appropriate optical theorems. The kinematic structure also leads to a signature rule, for the (a) type triple discontinuities, that the product of signatures in the three regge channels must be positive. (We believe that this signature rule will ultimately lead to the even signature property of the pomeron when we finally extract the physical S-Matrix from reggeon diagrams.) The analytic properties leading to this signature rule also imply that for the lowest-order triple-regge amplitudes containing the anomaly, triple and double discontinuities are trivially related. It is thus possible to evaluate all triple-regge anomaly contributions to (22) by evaluating double discontinuities.

Figs. 2(a) and (b) are, respectively, double discontinuities in $(s_{13}, s_{2'3'})$ and $(s_{23}, s_{1'3'})$, where $s_{ij} = (P_i + P_j)^2$ for $i, j = 1, 2, 3, 1', 2', 3'$. Since we are looking for the anomaly we ignore gluon self-interactions and so argue, as follows, that the twelve diagrams of Fig. 8 are all the lowest-order contributions to the $(s_{13}, s_{2'3'})$ double discontinuity (the hatched lines are again on-shell).

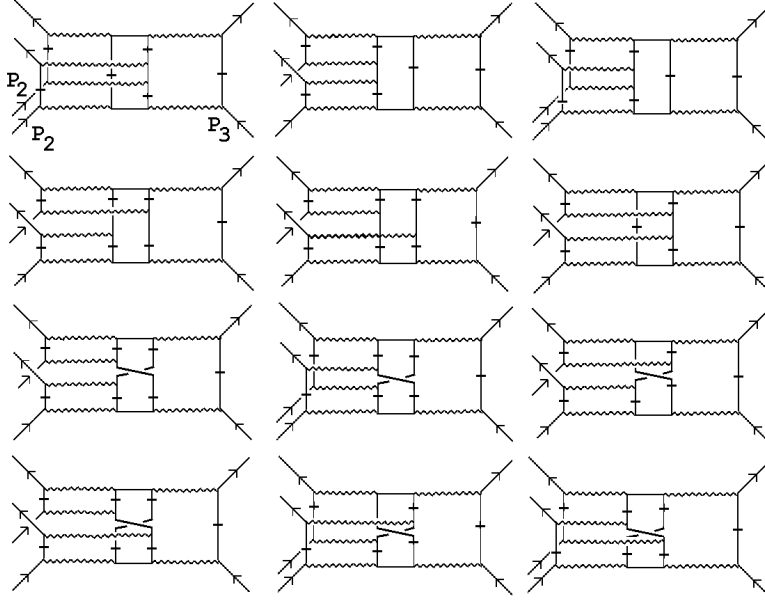


Fig. 8 Contributions to the $(s_{13}, s_{2'3'})$ Double Discontinuity.

The initial scattering process producing the s_{13} intermediate state is necessarily the production of a quark-antiquark pair. Without loss of generality, we can draw this process as in the bottom part of all the diagrams (since we sum over directions on the exchanged quark line). Similarly the $s_{2'3'}$ intermediate state is associated with the reverse of this production process. The quark loop obtained by joining the amplitudes for these initial and final scatterings is either planar or it has a twist. The six diagrams of each kind are obtained by attaching the two gluons that do not participate in either the initial or final scattering process, in all possible ways.

We recognize the first diagram in Fig. 8 as that of Fig. 2(a). It can be shown[1] that none of the remaining eleven diagrams contain both the necessary tensor structure and the corresponding light-cone momenta needed for the anomaly divergence. Consequently the complete contribution of the anomaly is obtained by summing over the contributions of the form of Fig. 2(a) for each of the twenty-four possible combinations of initial and final subenergy discontinuities. The arguments that we gave above for the cancelation of the anomaly in the scattering of elementary quarks or gluons then apply.

In more complicated scattering processes anomaly interactions can appear without cancelation. As we discuss at greater length in [1], all the reggeon states involved must carry anomalous color parity. Such states appear when additional particles are produced (or absorbed) at the external vertices. Also, since anomaly vertices do not conserve color parity they have to appear pairwise. Although the anomaly produces an infra divergence in the reggeon interaction in which it appears, it does not produce divergences in full amplitudes because of compensating reggeon

Ward identity zeroes.

The anomaly does produce divergent amplitudes if some external couplings are chosen so that particular reggeon Ward identity zeroes are absent. An anomalous color parity “reggeon condensate” (with the quantum numbers of the winding-number current) can be introduced this way. It was argued in [3] that, in a color superconducting phase with the gauge symmetry broken from SU(3) to SU(2), this condensate is consistently reproduced in all reggeon states by anomaly infra-red divergences, while also producing confinement, chiral symmetry breaking and a regge pole pomeron. SU(3) gauge invariance should be obtained by critical pomeron behavior[9] in which the condensate and superconductivity simultaneously disappear. Having the full structure of the anomaly under control, we hope to implement the program of [3] in detail in future papers. If we obtain a unitary (reggeon) S-Matrix, as we anticipate, it will be very close to perturbation theory, with the non-perturbative properties of confinement and chiral symmetry breaking a consequence of the anomaly only.

References

- [1] A. R. White, ANL-HEP-PR-99-102
- [2] S. Coleman and B. Grossman, *Nucl. Phys.* **B203**, 205 (1982).
- [3] A. R. White, *Phys. Rev.* **D58**, 074008 (1998), see also Lectures in the Proceedings of the Theory Institute on Deep-Inelastic Diffraction, Argonne National Laboratory (1998).
- [4] P. Goddard and A. R. White, *Nucl. Phys.* **B17**, 1, 45 (1970).
- [5] A. R. White, *Int. J. Mod. Phys.* **A11**, 1859 (1991); A. R. White in *Structural Analysis of Collision Amplitudes*, proceedings of the Les Houches Institute, eds. R. Balian and D. Iagolnitzer (North Holland, 1976); H. P. Stapp *ibid.*
- [6] H. P. Stapp and A. R. White, *Phys. Rev.* **D26**, 2145 (1982).
- [7] V. N. Gribov, I. Ya. Pomeranchuk and K. A. Ter-Martirosyan, *Phys. Rev.* **139B**, 184 (1965).
- [8] E. A. Kuraev, L. N. Lipatov, V. S. Fadin, *Sov. Phys. JETP* **45**, 199 (1977); J. B. Bronzan and R. L. Sugar, *Phys. Rev.* **D17**, 585 (1978), his paper organizes into reggeon diagrams the results from H. Cheng and C. Y. Lo, *Phys. Rev.* **D13**, 1131 (1976), **D15**, 2959 (1977); V. S. Fadin and V. E. Sherman, *Sov. Phys. JETP* **45**, 861 (1978); V. S. Fadin and L. N. Lipatov, *Nucl. Phys.* **B477**, 767 (1996)

and further references therein; J. Bartels, *Z. Phys.* **C60**, 471 (1993) and further references therein; A. R. White, *Int. J. Mod. Phys.* **A8**, 4755 (1993).

- [9] A. A. Migdal, A. M. Polyakov and K. A. Ter-Martirosyan, *Zh. Eksp. Teor. Fiz.* **67**, 84 (1974); H. D. I. Abarbanel and J. B. Bronzan, *Phys. Rev.* **D9**, 2397 (1974).